Pergamon

Tetrahedron 55 (1999) 14435–14450

TETRAHEDRON

A New Ferrocenemethyl-thymidine Nucleoside: Synthesis, Incorporation into Oligonucleotides and Optical Spectroscopic Studies on the resulting Single Strand, Duplex and Triplex Structures.

Enrico Bucci,[2] Lorenzo De Napoli,[1] Giovanni Di Fabio,[1] Anna Messere,[1] Daniela Montesarchio,[1] Alessandra Romanelli,[2] Gennaro Piccialli[3*] and Michela Varra[4]

[1]*Dipartimento di Chimica Organica e Biologica, Università degli Studi di Napoli "Federico II", Via Mezzocannone 16, 80134 Napoli, Italy;*
[2]*Centro di Studio di Biocristallografia del CNR, Via Mezzocannone 4, 80134 Napoli, Italy;*
[3]*Università del Molise, Facoltà di Scienze, Via Mazzini 8, 86170 Isernia, Italy;*
[4]*Dipartimento di Chimica delle Sostanze Naturali, Via D. Montesano, 49, 80131 Napoli, Italy.*
FAX number: 39-081-5521217
e-mail: picciall@cds.unina.it

Received 25 June 1999; revised 14 September 1999; accepted 1 October 1999

Abstract. A new thymidine analogue, bearing a ferrocenemethyl residue at the N-3 position of the base, was synthesized in high yields *via* Mitsunobu reaction of ferrocenemethanol with sugar protected thymidine, converted into the corresponding 3'-phosphoramidite and incorporated into oligonucleotides. Duplex and triplex formation experiments, evaluated by UV and CD spectroscopy, showed a dramatic decrease of the affinity towards complementary single strands, while for triplexes, the introduction of a ferrocene residue in the third strand resulted in higher melting temperatures, associated with a reduced content of triplex structure.
© 1999 Elsevier Science Ltd. All rights reserved.

Keywords. Mitsunobu reaction; Ferrocenes; Solid phase synthesis; Nucleic Acids analogues; Circular Dichroism.

Introduction.

Iron-containing sandwich compounds are known to display a pronounced antitumoral activity,[1] with localization of the metal-bound species in the cell nucleus.[2,3] The biological properties of ferrocenyl derivatives, lacking apparent coordination sites,[1,3-7] have been postulated to involve non-covalent interactions with nucleic acids, [8] which is of great interest in the systematic design of non platinum-group metal antitumor drugs. [9-11] Recently several ferrocene derivatives functionalized with nucleobases[12,13] and nucleosides[13] have been synthesized in an effort to exploit their therapeutic potential. In addition to showing cytostatic and antitumoral activities, ferrocenyl derivatives were revealed to be useful tools in analytical applications,[14-15] *e.g.* as electrochemical probes for DNA or RNA targeting. It has been shown that ferrocene groups covalently bound

0040-4020/99/$ - see front matter © 1999 Elsevier Science Ltd. All rights reserved.
PII: S0040-4020(99)00889-3

to oligodeoxyribonucleotides (ODNs) can be used as extremely sensitive markers[16] to detect specific DNA and RNA targets as an alternative to hazardous and short-living radioisotopes.[17] Moreover 5'-ferrocene conjugated ODNs have been found to show enhanced affinity towards double stranded DNA.[18] The incorporation of a ferrocenyl residue into ODNs has been achieved so far by coupling a ferrocenyl-phosphoramidite[19] derivative with the 5'-OH end of the oligonucleotide chain: alternatively the condensation of an activated ester of ferrocene-carboxylic acid[14,18] with a 5'-amino modified end of the ODN chain has also been reported. A key advantage in the procedures described is that, by attaching a conjugating molecule at the 5'-terminus of an oligomer, no modification in the standard automated solid phase synthesis[20,21] protocols has to be introduced. On the other hand, the cited syntheses allow uniquely terminal derivatizations of oligonucleotide chains with the conjugating molecule; these studies therefore furnish only a partial insight into the influence of a ferrocene probe on the base stacking and on the DNA hydrogen bonds base recognition mechanism. In this frame and in an effort to study the binding properties of metallocene-ODN conjugates we focused our attention on the preparation of a suitably functionalized nucleoside, covalently linked through the base to a ferrocene unit, which could be inserted in any desired position of the ODN chain *via* a fully automated synthetic procedure.[20,21]

Herein we report an easy and high yielding one pot synthesis of a new thymidine derivative linking a ferrocenemethyl residue at the N-3 position of the base, which was then converted into the corresponding 3'-phosphoramidite derivative and inserted in biologically interesting DNA sequences. Two 17-mers of general sequence $^{5'}$CTGCTAGAGATTTTTAC$^{3'}$, differing in the ferrocenemethyl-thymidine position (**a** and **b**, Figure 1), were synthesized to target in an antisense approach[22] a tract of the PBS binding region of HIV-1 genomic RNA.[23] Moreover the triplex forming ability of the 16-mers of sequence $^{5'}$TCTCTCTCTCTCTCTC$^{3'}$ (**c** and **d**, Figure 1) with one ferrocenemethylthymidine residue at two different positions, was studied by quantifying triplex formation in the presence of the 16 bp $(AG)_8/(TC)_8$ duplex (**III**, Figure 1), a repeating sequence found in human genome[24] often investigated for antigene therapy.[25]

UV thermal analysis and CD spectroscopy were used to investigate the affinity of the studied sequences towards the corresponding single stranded or duplex targets and to elucidate the ferrocene effect on the solution structure of the resulting double (for **a** and **b**) or triple (for **c** and **d**) helical complexes.

Results and Discussion.

Synthesis of ferrocenyl-nucleoside 4.

Although *N*-alkylations of nucleosides have been widely described,[26] introduction of an alkyl group directly onto a nucleobase always constitutes a challenging task. Compound **3** (Scheme 1) was efficiently prepared coupling nucleoside **1** with ferrocenemethanol (**2**) by a Mitsunobu reaction.[27] Commercially available ferrocenemethanol **2**, previously activated through the classical redox Mitsunobu system DEAD-TPP, reacted with the N-3 position of the thymine base affording derivative **3** in 45 % yield. Higher yields were obtained using the alternative Mitsunobu system[28] tributylphosphine (TBP)/1,1'-(azodicarbonyl)dipiperidine (ADDP).

Treating ferrocenemethanol **2** (1.5 eq) and 5'-*O*-(4,4'-dimethoxytriphenylmethyl)-3'-*O*-acetyl-thymidine **1** (2 eq) with TBP (2.5 eq) and ADDP (2.5 eq) according to a described procedure,[28] compound **3** was obtained in 85 % yield. Moreover with the introduction of the redox system ADDP/TBP the formation of side products (alkylated hydrazine derivatives) decreased, thus simplifying the purification of **3**. The structure of **3** was confirmed by spectroscopic data. Particularly the ^{13}C NMR spectrum showed a signal at 40.2 ppm, diagnostic of the insertion of the ferrocene-CH_2 group in the N-3 position of the base, thus excluding *O*-alkylation products. Attempts to obtain the O-4 ferrocene-linked derivative reacting 4-chloro,3',5'-di-*O*-acetylthymidine[29] with ferrocenemethanol, previously treated with strong bases (DBU, NaH, butyllithyum), failed in the conditions tested, leading exclusively to the corresponding N-3 derivative. This regiochemistry is not easily explainable since it is well known that C-4 activated thymidines react with N- and O-nucleophiles giving 4-substituted derivatives in high yields[30,31] and could therefore be accounted for by initial O-4 addition undergoing an O→N migration. Treatment of **3** with NH_4OH/CH_3OH (3:2, v/v) at 50 °C for 12 h led to **4** in almost quantitative yields; this confirmed the stability of the ferrocene-thymine linkage to the alkaline conditions required for the final oligonucleotides deprotection. Compound **4** was successively phosphitylated in a standard manner[20] by reaction with 2-cyanoethyl-N,N-diisopropylchlorophosphoramidite (1.5 eq) and diisopropylethylamine (DIEA, 4 eq) in anhydrous CH_2Cl_2 (30 min, r.t.) to give **5** in 70 % yield after HPLC purification. The identity and purity of compounds **3** and **4** have been ascertained by HRFAB-MS and ^1H- and ^{13}C-NMR data, while ^1H-, ^{13}C- and ^{31}P-NMR data have confirmed the structure and purity of derivative **5**.

Scheme 1

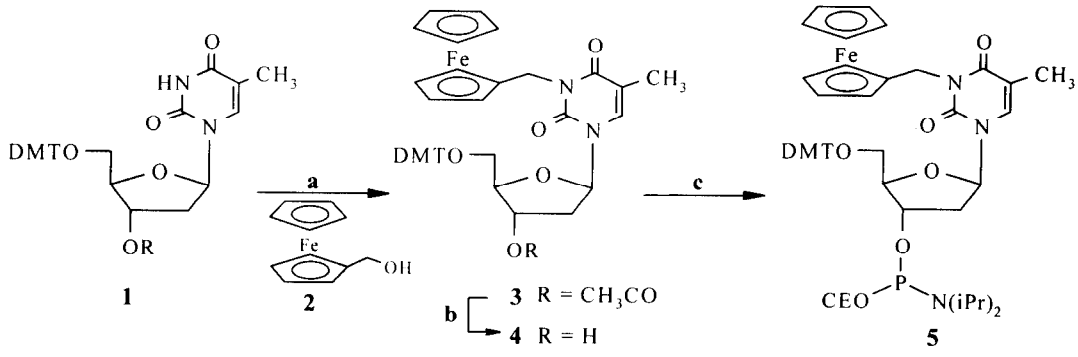

R = CH_3CO
DMT = 4,4'-dimethoxytriphenylmethyl
CE = CH_2CH_2CN

Reagents and conditions: a: **1** (2.0 eq), **2** (1.5 eq), P(*n*-but)$_3$ (2.5 eq), ADDP (2.5 eq), benzene, r.t. 12 h, 85 %. **b:** conc. NH_4OH/CH_3OH (3:2, v/v), 50 °C, 12 h, 98 %. **c:** 2-cyanoethyl-N,N-diisopropyl-chlorophosphoramidite (1.5 eq), DIEA (4.0 eq), CH_2Cl_2, r.t., 15 min, 70 % after HPLC purification.

Synthesis of ferrocene containing oligonucleotides.

Ferrocenemethyl-thymidine-3'-phosphoramidite **5** was inserted in the indicated positions of sequences **a-d** (Figure 1). All the oligonucleotides were synthesized on an automated DNA synthesizer following standard phosphoramidite procedures[20,21] on a 5 μmol scale, using **5** and commercially available 3'-*O*-(2-cyanoethyl)-*N,N*-diisopropylphosphoramidite nucleosides as building blocks in concentration of 40 mg/mL. In all cases coupling efficiencies were found to be in the range 98-99 %, as judged by 4,4'-dimethoxytriphenylmethyl (DMT) cation tests. The oxidation steps of the DNA synthesis involved the momentary oxidation of Fe^{2+} to Fe^{3+}; nevertheless this process has not been further investigated because, as already described,[19] the green colour species Fe^{3+} quickly returned to yellow-orange Fe^{2+}. Detachment from the support and total deprotection of the synthesized oligomers were achieved by aq. ammonia treatment for 16 h at 55 °C. Crude materials were analyzed and purified by ion exchange HPLC on a Partisil 10 SAX column. The isolated oligomers were desalted by gel filtration and their purity checked by reverse phase HPLC analysis. Oligomers **a**, **b**, **c** and **d** were analyzed by MALDI-TOF mass spectrometry, giving in all cases masses in accordance with those calculated for the corresponding molecular ions $(M - H)^-$.

Figure 1

Synthesized oligonucleotides **a,b,c,d**; **a**, **b** complexes with target DNA single strands **(I+a)**, **(I+b)**; **a**, **b** complexes with target RNA single strands **(II+a)**, **(II+b)**; **c**, **d** complexes with target double stranded DNA **(III+c)**, **(III+d)**.

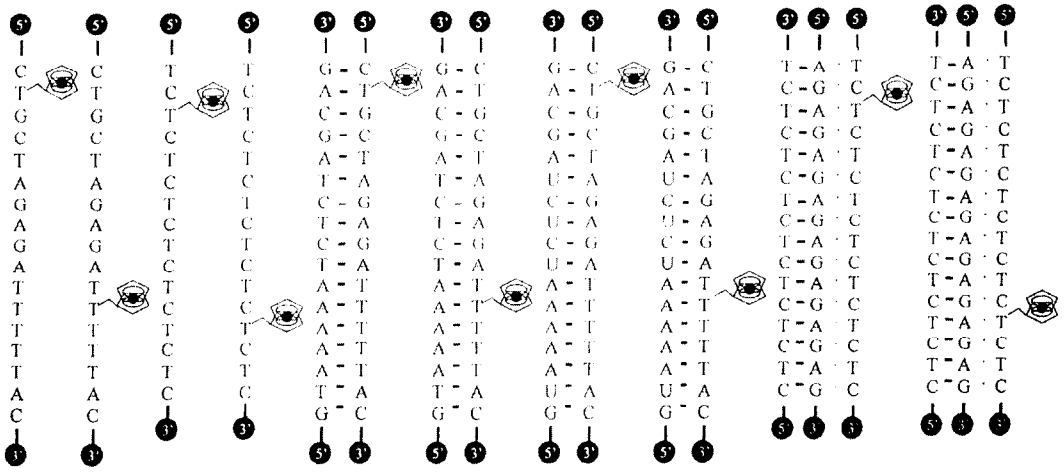

Spectroscopic and Thermodynamic Studies.

CD spectra obtained for sequences **a** and **b**, compared to the ones obtained for the corresponding ferrocene-free single stranded DNA, are reported in Figure 2. As apparent from the reduced absorption intensity

at 280 nm, the general effect of the insertion of a ferrocene residue on single stranded DNA fragments is a reduction of intra-strand base stacking probably due to the steric hindrance of ferrocene-thymidine. Surprisingly, this effect is particularly pronounced in **a**, where the ferrocene is near the 5'-end of the strand, and less evident in **b**, where the ferrocene is in the middle of the sequence. This unexpected pattern may be related to a different local base composition around the ferrocenyl-thymidine in **a** and **b**. In particular, it is possible that ferrocenyl-thymidine makes more unfavourable steric clashes when adjacent to G as in sequence **a**; on the contrary, in sequence **b** the modified thymidine is surrounded only by T's and may thus protrude out of the

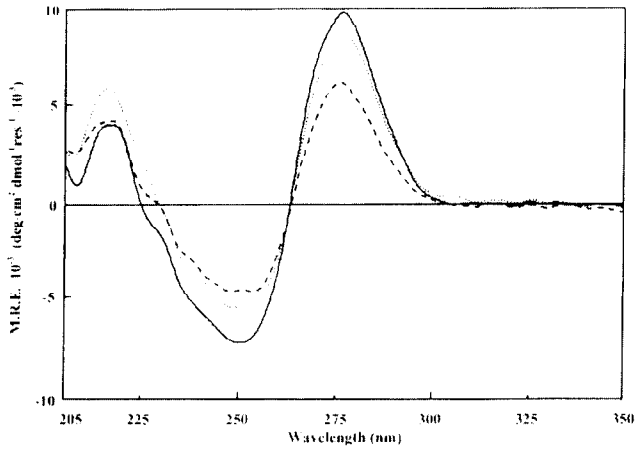

Figure 2.
Molar residue ellipticity (region 205-350 nm) of 17-mers ferrocene-free (continuous line), **a** (hatched line) and **b** (dotted line) single strand oligonucleotides, 2.0 μM in aq. 100 mM NaCl, 10 mM NaH_2PO_4 at pH 7.0.

intra-strand stacked pile of bases. In this hypothesis, it is not surprising that sequence **a** CD spectrum seems to be related to the one of a pentathymidine, which points in favour of a local unstacking in the 5'-tract.

For duplex formation studies UV thermal denaturation experiments and CD spectra were carried out mixing the modified ODN (**a** or **b**) with the corresponding target (ssDNA **I** or ssRNA **II**) in 1:1 ratio in a 100 mM NaCl, 10 mM NaH_2PO_4, aq. solution, at pH = 7.0. UV monitored thermal denaturation kinetics of duplex **(I+a)**, duplex **(I+b)** and of the corresponding ferrocene-free duplex are reported in Figure 3 and the corresponding Tm's, calculated as the maxima of the first derivative plots of absorbance *vs.* temperature, are summarized in Table 1.

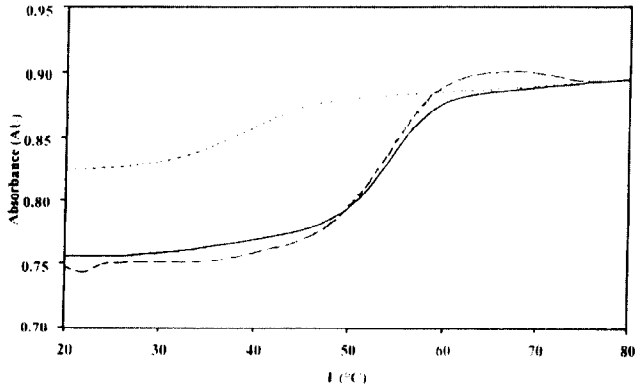

Figure 3.
UV melting profiles of 17-mers ferrocene-free (continuous line), **(I+a)** (hatched line) and **(I+b)** (dotted line) double stranded oligonucleotides, 2.0 μM each strand in aq. 100 mM NaCl, 10 mM NaH_2PO_4 at pH 7.0.

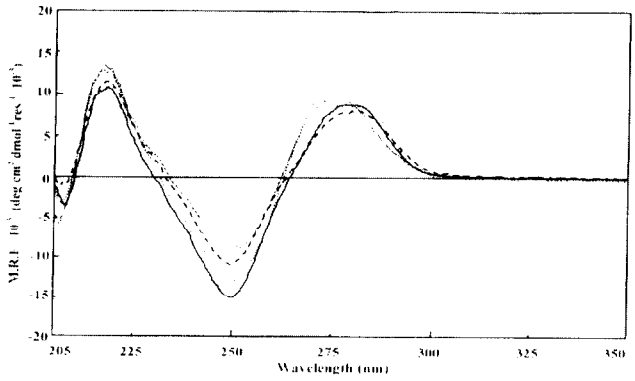

Figure 4.
Molar residue ellipticity (region 205-350 nm) of 17-mers ferrocene-free (bold continuous line), **(I+a)** (bold hatched line) and **(I+b)** (bold dotted line) double stranded oligonucleotides, 2.0 μM each strand in aq. 100 mM NaCl, 10 mM NaH_2PO_4 at pH 7.0. The sum spectra of the corresponding single strands are also reported (ferrocene-free single strand sum, thin continous line; single strands **a**, **I** sum thin hatched line; single strands **b**, **I** sum thin dotted line).

Table 1.

	Tm modified	$\Delta Tm_{(modified-unmodified)}$
I+a	**52.2**	**-0.4**
I+b	**38.5**	**-14.1**
II+a	**48.3**	**-7.7**
II+b	**41.3**	**-14.7**
III+c (pH=5.5)	**62.0**	**+1.0**
III+d (pH=5.5)	**66.0**	**+5.0**
III+c (pH=6.0)	**55.0**	**+4.0**
III+d (pH=6.0)	**57.0**	**+6.0**

I: DNA compl.: $^{5'}$GTAAAAATCTCTAGCAG$^{3'}$
II: RNA compl.: $^{5'}$GUAAAAAUCUCUAGCAG$^{3'}$
III: Duplex compl. : $^{5'}$AGAGAGAGAGAGAGAG$^{3'}$
$^{3'}$TCTCTCTCTCTCTCTC$^{5'}$

A strong destabilization of duplex **(I+b)** is clearly evident, with a reduction of base-pairing and cooperativity of the melting transition, and a relative absence of effect for duplex **(I+a)** with respect to the ferrocene–free duplex. We infer that the presence of a ferrocenyl-thymidine in the 5'-terminal position of **a** in duplex **(I+a)** did not produce a substantial modification on neighbour base pairing, which is not unexpected, because of the ferrocene localization on the flexible end of the duplex. Incorporation of a ferrocenyl-nucleotide in the middle of the sequence dramatically affects the Tm of the target duplex **(I+b)**. CD spectra gave information consistent with those derived from UV thermal analysis. CD spectra for duplex **(I+a)**, duplex **(I+b)** and the ferrocene-free duplex are reported in Figure 4 in comparison with the corresponding normalized sums of the single strand spectra. Again, duplex **(I+b)** shows the most relevant change with respect to the ferrocene-free duplex. As evident from Figure 4, all the denaturated-form CD spectra exhibit a blue shift in the 280 nm band, a less intense 250 nm band and a more intense 215 nm band. Duplex **(I+a)** CD spectrum shows minor

changes in the 280 nm band (and thus minor base-stacking differences) and no changes in the 215 nm band with respect to the natural duplex. Only the 250 nm band is different if compared to the related band of the ferrocene-free duplex spectrum. It seems therefore that the effect of ferrocene introduction in **(I+a)** is a small, local rearrangement of the duplex structure. Duplex **(I+b)** CD spectrum shows a blue-shift and an intensity increase in the 280 nm band, an intensity decrease at 250 nm and an intensity increase at 215 nm. All this evidence points to an extensive denaturation of duplex **(I+b)**, but the 280 nm band is far more intense than expected also for complete denaturation [as evident from the denatured-form spectrum of duplex **(I+b)**]. These results may be explained by a local ferrocene mediated denaturating effect on the duplex, with the poly-thymidine tract denatured and most part of the G·C paired. This combination would give the maximum intensity in the 280 nm band because, as previously reported,[32] the A·T unpairing causes a strong increase in the 280 nm band.

As in the case of duplex DNA\DNA, a B-like double helix, also the hybrid duplex RNA\DNA, which is an A-like structure, was investigated for its ability to accomodate a ferrocenyl-thymidine by means of CD spectroscopy and UV monitored melting experiments. The same sequences used for single strands experiments were examined in the presence of complementary RNA strand **II** for their ability to form a hybrid duplex.

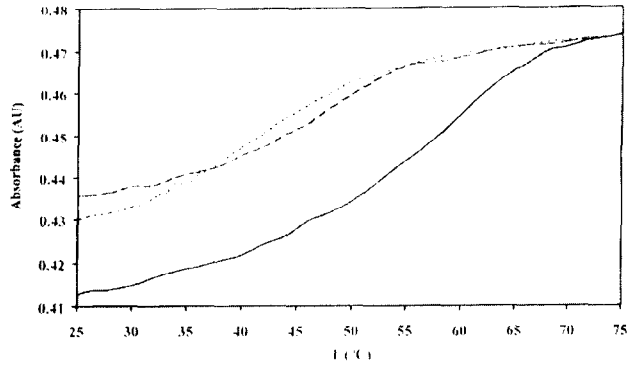

Figure 5.
UV melting profiles of 17-mers ferrocene-free (continuous line), **(II+a)** (hatched line) and **(II+b)** (dotted line) DNA/RNA hybrid double stranded oligonucleotides, 2.0 μM each strand in aq. 100 mM NaCl, 10 mM NaH_2PO_4 at pH 7.0.

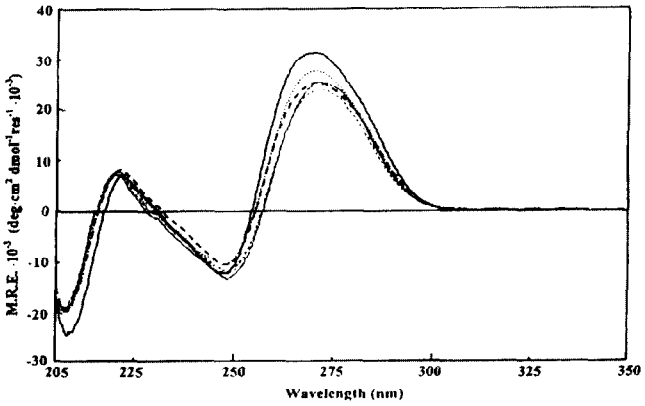

Figure 6.
Molar residue ellipticity (region 205-350 nm) of 17-mers ferrocene-free (bold continuous line), **(II+a)** (bold hatched line) and **(II+b)** (bold dotted line) DNA/RNA hybrid double stranded oligonucleotides, 2.0 μM each strand in aq. 100 mM NaCl, 10 mM NaH_2PO_4 at pH 7.0. The sum spectra of the corresponding single strands are also reported (ferrocene-free single strand sum, thin continous line; single strands **a**, **II** sum thin hatched line; single strands **b**, **II** sum thin dotted line).

UV monitored thermal denaturation kinetics of hybrid **(II+a)**, hybrid **(II+b)** and of the corresponding ferrocene-free hybrid are reported in Figure 5, while the corresponding Tm's are reported in Table 1. It is immediately evident that, in the case of an A-like double helix, a strong perturbation is obtained even if the ferrocene residue is at the end of the duplex. This observation may be explained as a consequence of the reported intrinsic structural rigidity[33] of the A-type double helix. The low flexibility of an A-like double helix may probably not allow to compensate for the ferrocene-induced structural perturbation even in duplex **(II+a)**, in contrast to the corresponding **(I+a)** double helix. CD spectra for hybrid **(II+a)**, hybrid **(II+b)** and ferrocene-free hybrid are reported in Figure 6 in comparison with the corresponding normalized sums of the single strand spectra. As evident from the ferrocene-free duplex and denatured spectra, denaturation of A-form causes a 275 and 207 nm band intensity decrease. The 207 nm band of all spectra, apart from the ferrocene-free hybrid, is strikingly similar, thus suggesting an extensive denaturation for hybrids **(II+a)** and **(II+b)**. The 275 nm band of hybrid **(II+a)** is similar to the corresponding band of all-denatured **(II+a)**, while hybrid **(II+b)** still shows some differences with respect to the band of all-denatured hybrid **(II+b)**. This effect, as for the corresponding DNA/DNA duplex, may result from the local $(T{\cdot}A)_5$ denaturation caused by the ferrocene residue.

For triplex investigations oligomer **c** (or **d**) was mixed with the corresponding target duplex **III** in 1:1 ratio in a 140 mM KCl, 5 mM NaH_2PO_4, 5 mM $MgCl_2$ aq. solution at acidic pH values (5.5, 6.0) to test for ferrocene effects in the presence of different protonation states of the cytosines. Thermal stability of the studied triplexes was first investigated by UV-monitored thermal denaturation. Normally, UV melting experiments of triple-helices result in a biphasic strand dissociation according to the transitions triplex → duplex + one single strand → three single strands. In some cases, however, it is only possible to recognize a single transition, as we observed in accord with reported melting data for the studied sequences.[34] This monophasic transition is not turned into a biphasic one by the presence of one ferrocenyl-thymidine residue in triplex **(III+c)** and **(III+d)** in the examined pH range, so that it is not possible, by UV-data, to clarify if a stable triple helix melting together with the duplex has been formed in the presence of ferrocene (data not shown).

To assess for the triplex presence, CD experiments were performed. CD spectra for triplex **(III+c)**, **(III+d)** and ferrocene-free triplex are reported in Figures 7 and 8 for pH 5.5 and 6.0, respectively, in comparison with the corresponding normalized sums of the single strands spectra.

It is clear from the reported CD spectra that in the presence of the Hoogsteen strand a transition toward a triplex form is common to all the examined ODNs. In particular, the 220 nm band, diagnostic for triplex formation in polymers of the same sequence,[35,36] becomes deeper if compared to the corresponding band in the normalized sum spectra and the 280 nm band decreases in intensity and shows a red shift. Moreover, spectra obtained for the normalized sums and spectra obtained for **(III+c)**, **(III+d)** and for the ferrocene-free triplex share at least one common isodichroic point at any pH examined, in agreement with the hypothesis that triplexes **(III+c)** and **(III+d)** uniquely differ from the ferrocene-free triplex in the lower content of triplex and the higher content of single strands, thus excluding the possibility of very different structures induced by the ferrocene residue.

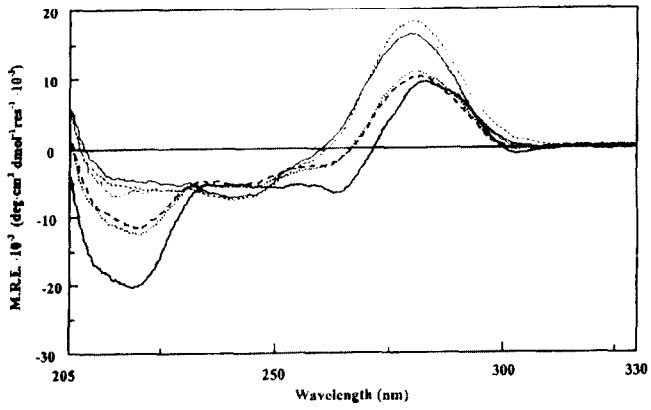

Figure 7.
Molar residue ellipticity (region 205-350 nm) of 16-mers ferrocene-free (bold continuous line), (**III+c**) (bold hatched line) and (**III+d**) (bold dotted line) triplex oligonucleotides, 1.2 μM each strand in aq. 140 mM KCl, 5 mM NaH_2PO_4, 5mM $MgCl_2$ at pH 5.5. The sum spectra of the corresponding single strand + duplex are also reported (ferrocene-free single strand + duplex sum, thin continous line; single strand **c**, duplex **III** sum thin hatched line; single strands **d**, duplex **III** sum thin dotted line).

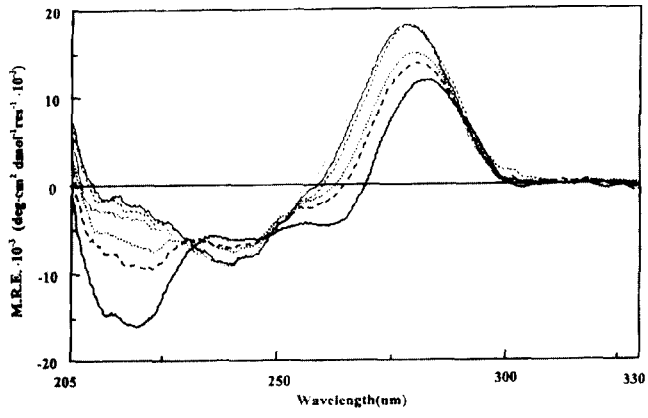

Figure 8.
Molar residue ellipticity (region 205-350 nm) of 16-mers ferrocene-free (bold continuous line), (**III+c**) (bold hatched line) and (**III+d**) (bold dotted line) triplex oligonucleotides, 1.2 μM each strand in aq. 140 mM KCl, 5 mM NaH_2PO_4, 5mM $MgCl_2$ at pH 6.0. The sum spectra of the corresponding single strand + duplex are also reported (ferrocene-free single strand + duplex sum, thin continous line; single strand **c**, duplex **III** sum thin hatched line; single strand **d**, duplex **III** sum thin dotted line).

To quantitatively analyze the CD-observed triplex-content variation, the CD spectra obtained were fitted with an *ad hoc* set of basis spectra previously reported[37] using a standard linear deconvolution method. We obtained triplex content percentages for ferrocene-free, **(III+c)** and **(III+d)** triplexes respectively of 93, 67 and 64 % at pH 5.5 and 73, 45 and 38 % at pH 6.0. The difference between the calculated CD spectra and the measured ones was never greater than 1 %. This evidence indicates that the ferrocenyl-thymidine causes a similar effect on triplex content decrease irrespective of its position in the triplex forming oligonucleotide (TFO) sequence and pH value. To evaluate the stability of the triplexes under investigation *via* CD-monitored melting experiments, we looked for a selected wavelength λ where:

$$[\theta]_\lambda \text{duplex} + [\theta]_\lambda \text{ss} = 3[\theta]_\lambda \text{ss} \neq [\theta]_\lambda \text{triplex}$$

with:

$[\theta]_\lambda$ss representing the molar ellipticity for the single strand at wavelength λ;

$[\theta]_\lambda$duplex the molar ellipticity for the duplex at wavelength λ;

$[\theta]_{\lambda}$triplex the molar ellipticity for the triplex at wavelength λ;

In our case this condition is best verified for λ = 220 nm. Obtained CD monitored thermal denaturation kinetics at pH 5.5 and 6.0 are reported in Figure 9 as CD *vs.* temperature plots with the corresponding first derivatives profiles (Figure 10).

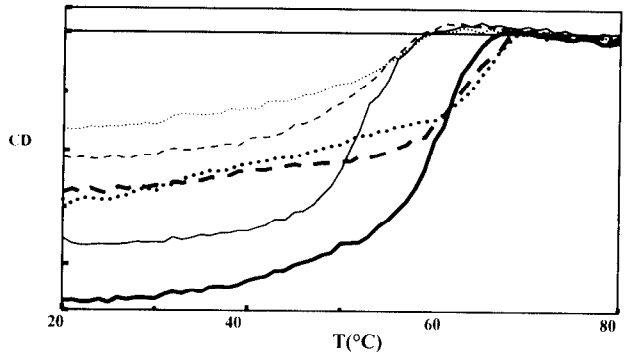

Figure 9.
CD melting profile of 16-mers ferrocene-free (continuous line), **(III+c)** (hatched line) and **(III+d)** (dotted line) triplex oligonucleotides, 1.2 μM each strand in aq. 140 mM KCl, 5 mM NaH_2PO_4, 5mM $MgCl_2$ at pH 5.5 (bold lines) and at pH 6.0 (thin lines).

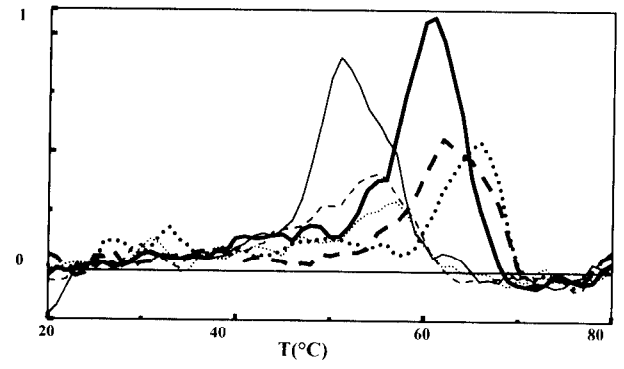

Figure 10.
First derivative profiles of CD melting of 16-mers ferrocene-free (continuous line), **(III+c)** (hatched line) and **(III+d)** (dotted line) triplex oligonucleotides.

When the ferrocenyl-thymidine is present, we observed in any case a reduction of the CD *vs.* temperature plots intensity and of the thermal variation for the denaturation process, in agreement with the triplex content decrease previously derived from CD spectra. Moreover, a loss of cooperativity in the melting process is evident as an increase of the temperature interval where the melting occurs and a decrease of the CD *vs.* temperature plot slope in the same region. The melting temperatures, calculated as the maxima of the first derivative plots of CD at 220 nm *vs.* temperature, are summarized in Table 1.

It is immediately evident that the ferrocenyl-thymidine presence enhances the Tm's of the formed triplexes even if the total triplex content is lower. These data may be explained assuming a loss of Hoogsteen base pairings in triplexes **(III+c)** and **(III+d)** caused by the ferrocene introduction in TFOs **c** and **d**, balanced by favourable interactions of the ferrocene moiety with target duplex **III**. A thermal stabilization effect produced by a ferrocene residue has also been previously found[18] on different ferrocene-conjugated TFOs where the

ferrocene unit was linked at the 5'-end *via* an aminohexamethylene spacer. Therefore it is reasonable to hypothesize that the denaturated region of the ferrocene-containing TFO in the triplex complex can act as a sufficiently flexible linker to favourably accomodate the ferrocene residue.

Further studies to elucidate the mechanism of triplex stabilization mediated by the ferrocene unit linked to TFOs are currently in progress.

Conclusions.

An easy and convenient synthetic route to obtain 3-N-ferrocenemethyl-thymidine derivative **3** by Mitsunobu reaction of ferrocenemethanol with 5'-O-(4,4'-dimethoxytriphenylmethyl)-3'-O-acetyl-thymidine has been developed and its incorporation into two biologically relevant ODN sequences has been achieved.

Ferrocenyl 17-mers **a** and **b** and 16-mers **c** and **d** were efficiently synthesized, purified by HPLC and characterized by MALDI-TOF MS spectrometry. **a** and **b** were shown, by CD and UV thermal analysis, to be able to hybridize complementary DNA and RNA single strands, even if with reduced affinity, whereas **c** and **d** resulted in stable triplex structures when mixed with double stranded DNA. In particular, by means of UV and CD experiments we found that the presence of a ferrocene unit:

a) perturbed single strands stacking to a variable extent depending on the sequence context;
b) dramatically affected double strands pairing, except when the ferrocenemethyl-thymidine is terminal in a B-DNA duplex, even if in any studied case a duplex structure is indeed formed;
c) measurably reduced triplex formation, but caused a notable increase in the corresponding Tm.

It is evident that, even if applications[9-19] of a ferrocene-thymidine containing ODN to target a single strand are not precluded, the characteristics of the proposed ferrocene-functionalized nucleoside especially support its insertion in specific TFOs to exploit the ferrocene potential as electrochemical probe for extremely sensitive detections of double stranded DNA. This point is particularly relevant in all the applications concerned with the specific recognition of oligonucleotide sequences *in vivo*, where the target is often a nucleic acid in duplex form.

Experimental Section.

General Methods.

Ferrocenemethanol was purchased from Aldrich. Column chromatography was performed on silica gel (Merck, Kieselgel 40, 0.063-0.200 mm). FAB mass spectra (positive) were determined on a ZAB 2SE spectrometer. MALDI TOF mass spectra (negative ion) were performed on a Kratos Compact Maldi IV spectrometer using 3-hydroxypicolinic acid as matrix. NMR spectra were recorded on Bruker WM-400 and on Varian- Gemini 200 spectrometers. All chemical shifts are expressed in ppm with respect to the residual solvent signal. *J* values are given in Hz. The functionalized CPG support (loading 100-110 μmol/g) was purchased from Millipore. The oligonucleotides were assembled on a Millipore Cyclone Plus DNA synthesizer, using commercially available 3'-*O*-(2-cyanoethyl)-*N*,*N*-diisopropylphosphoramidite nucleosides as building blocks.

HPLC analyses were carried out on a Beckman System Gold instrument equipped with a UV detector module 166 and a Shimadzu Chromatopac C-R6A integrator. UV measurements were performed on a Perkin Elmer Lambda 7 spectrophotometer. Thermal denaturation experiments were run on a Cary 1E Varian spectrophotometer equipped with a Haake PG20 thermoprogrammer at λ = 260 nm. CD spectra were run on a Jasco J-715 spectropolarimeter equipped with a Jasco PTC-348W1 thermoprogrammer, and carried out at λ = 220 nm for CD melting experiments. Melting points were determined on a Reichert Thermovar apparatus and are uncorrected.

Synthesis of 3–*N*–ferrocenemethyl-5'–*O*-(4,4'-dimethoxytriphenylmethyl)-3'–*O*-acetyl-thymidine (3).

500 mg (0.85 mmol) of 5'-*O*-(4,4'-dimethoxytriphenylmethyl)-3'-*O*-acetyl-thymidine (**1**) were left in contact with 138 mg (0.64 mmol) of ferrocenemethanol (**2**) and 0.262 mL (1.06 mmol) of tributylphosphine (TBP) in anhydrous benzene (3.0 mL). The solution was stirred and cooled at 0 °C and 268 mg (1.06 mmol) of 1,1'-(azodicarbonyl)dipiperidine (ADDP) were added. After 15 min the reaction mixture was heated at r. t. and left stirring for 12 h. The crude material, concentrated under reduced pressure, was chromatographed on a silica gel column eluted with ethyl acetate in cyclohexane containing 0.5 % (v/v) of pyridine. Fractions eluted with cyclohexane/ethyl acetate 7:3 (v/v), collected and taken to dryness, afforded 565 mg (0.72 mmol, 85 % yield) of nucleoside **3**.

3: yellow solid, m.p. 95-97 °C. R_f = 0.7 (eluent benzene/ethyl acetate 85:15, v/v). $[\alpha]_D^{20}$ +12.2 (*c* 1.4, $CHCl_3$). ν_{max} (liquid film) 3425, 2937, 1743, 1707, 1675, 1646, 1513, 1470, 1251, 1179, 1039, 758 cm^{-1}. λ_{max} ($CHCl_3$)/nm 242 (23250) and 265 (15680). δ_H ($CDCl_3$, 200 MHz): 7.45 (1H, s, H-6); 7.28-6.68 (13H, complex signals, DMT); 6.36 (1H, dd, J=6.3 and 6.2, H-1'); 5.31 (1H, m, H-3'); 4.78 (2H, s, H-3 and H-4 ferrocenyl ring A); 4.36 (2H, s, H-2 and H-5 ferrocenyl ring A); 4.08 (5H, s, ferrocenyl ring B); 3.99 (3H, bs, CH_2-N-3 and H-4'); 3.68 (6H, s, OCH_3 DMT); 3.33 (2H, m, H_2-5'); 2.30 (2H, m, H_2-2'); 1.97 (3H, s, CH_3CO); 1.29 (3H, s, CH_3-5). δ_C ($CDCl_3$, 100 MHz): 170.0, 158.7, 135.3, 132.2, 130.0, 128.1, 127.9, 127.1, 113.2, 87.0, 163.0, 150.8, 144.1, 110.9, 84.9, 83.7, 82.3, 75.3, 70.6, 68.6, 68.0, 63.6, 55.2, 40.2, 38.0, 20.9, 12.3. HRMS (FAB) m/z $(M+H)^+$ found 785.2528. $C_{44}H_{44}FeN_2O_8 + H^+$ requires 785.2525.

Synthesis of 3–*N*–ferrocenemethyl-5'–*O*-(4,4'-dimethoxytriphenylmethyl)-thymidine (4).

Compound **3** (565 mg, 0.72 mmol) was treated with 10 mL of conc. aq. ammonia/CH_3OH (3:2, v/v) and heated at 50 °C for 12 h. The solution, dried *in vacuo*, was purified on a silica gel column eluted with increasing amounts of ethyl acetate in benzene (from 0 to 10 %) containing 0.5 % pyridine (v/v) to give pure **4** (390 mg, 0.71 mmol, 98 % yield).

4: yellow solid, m.p. 100-102 °C. R_f = 0.2 (eluent benzene/ethyl acetate 85:15, v/v). $[\alpha]_D^{20}$ +48.9 (*c* 0.41, $CHCl_3$). ν_{max} (liquid film) 3440 (broad), 2937, 1704, 1668, 1635, 1510, 1466, 1254, 1179, 1035, 755 cm^{-1}. λ_{max} ($CHCl_3$)/nm 242 (21800) and 265 (13600). δ_H ($CDCl_3$, 200 MHz): 7.49 (1H, s, H-6); 7.28-6.80 (13H, complex signals, DMT); 6.40 (1H, dd, J=6.3 and 6.2 Hz, H-1'); 4.88 (2H, s, H-3 and H-4 ferrocenyl ring A); 4.53 (1H,

m, H-3'); 4.45 (2H, s, H-2 and H-5 ferrocenyl ring A); 4.06 (5H, s, ferrocenyl ring B); 4.04 (2H, complex signals, $C\underline{H}_2$-N-3); 4.01 (1H, m, H-4'); 3.77 (6H, s, OCH_3 DMT); 3.50-3.30 (2H, m, H_2-5'); 2.32 (2H, m, H_2-2'); 1.46 (3H, s, CH_3-5); δ_C ($CDCl_3$, 100 MHz): 158.5, 135.2, 133.4, 129.9, 127.9, 127.8, 127.0, 113.1, 86.7, 163.0, 150.6, 144.2, 110.3, 85.8, 85.1, 82.4, 72.0, 70.4, 68.4, 67.9, 63.3, 55.1, 40.9, 40.1, 12.4. HRMS (FAB) m/z $(M+H)^+$ found 743.2426. $C_{42}H_{42}FeN_2O_7 + H^+$ requires 743.2420.

Synthesis of 3-*N*–ferrocenemethyl-5'–*O*-(4,4'-dimethoxytriphenylmethyl)-3'–*O*-(2-cyanoethyl)-*N*,*N*–diisopropylphosphoramidite-thymidine (5).

To a stirred solution of 390 mg (0.71 mmol) of nucleoside **4** and 0.486 mL (2.84 mmol) of diisopropylethylamine dissolved in 1.0 mL of anhydrous CH_2Cl_2, 0.237 mL (1.06 mmol) of 2-cyanoethyl-N,N-diisopropyl-chlorophosphoramidite were added dropwise at room temperature. After 30 min the reaction was complete as monitored by TLC and anhydrous ethyl acetate (15 mL) was added. The solution was washed with a saturated NaCl solution (2 × 10 mL) and the organic layer was evaporated under reduced pressure to give a pale orange oil. The mixture was dissolved in anhydrous CH_3CN and purified by HPLC on a semipreparative Lichrosorb Si60 Hibar column (Merck, 2.2×25 cm, 7 μm), eluted with cyclohexane/ethyl acetate 7:3 (v/v), flow 1.5 mL/min, detection at λ = 260 nm), retention time: 16.0 min.

5: (as diastereoisomeric mixture) yellow solid, R_f = 0.30 and 0.35 (eluent cyclohexane/ethyl acetate 7:3, v/v). $[\alpha]_D^{20}$ +79.5 (*c* 1.2, CH_2Cl_2). ν_{max} (liquid film) 3461, 2973, 2185, 1707, 1671, 1649, 1513, 1466, 1254, 1183, 1039, 834 cm^{-1}. δ_H ($CDCl_3$, 200 MHz): 7.59 and 7.52 (1H, s's, H-6); 7.41-6.75 (13H, complex signals, DMT); 6.42 (1H, m, H-1'); 4.88 (2H, s, H-3 and H-4 ferrocenyl ring A); 4,60 (1H, m, H-3'); 4.46 (2H, s, H-2 and H-5 ferrocenyl ring A); 4.17 (7H, bs, ferrocenyl ring B and $OC\underline{H}_2CH_2CN$); 4.08 (2H, bs, CH_2-N-3); 3.78 (6H, s, OCH_3 of DMT); 3.70-3.30 (4H, H_2-5', H-4'and $C\underline{H}(CH_3)_2$); 2.60 and 2.40 (2H, t's, $OCH_2C\underline{H}_2CN$); 2.49-2.20 (2H, m, H_2-2'); 1.42 (3H, s, CH_3C-5); 1.15 and 1.04 (12H, d's, $CH(C\underline{H}_3)_2$. δ_C ($CDCl_3$, DEPT, 100 MHz): 133.4, 130.1, 128.2, 128.1, 127.9, 127.1, 113.2, 145.3, 85.5, 85.3, 73.8, 70.6, 68.5, 67.9, 63.1, 55.2, 43.3, 40.2, 40.2, 24.5, 24.5, 20.3, 12.4. δ_P ($CDCl_3$, 161.98 MHz): 151.0, 150.4. HRMS (FAB) m/z $(M)^+$ found 942.3509. $C_{51}H_{59}FeN_4O_8^+$ requires 942.3420.

Solid-Phase Synthesis of Natural and Modified Oligomers a-d.

The syntheses of oligos **a-d** were performed on a DNA synthesizer following a standard phosphoramidite procedure[20,21] (5 μM scale). Prefunctionalized CPG supports (45 mg, 0.10 mmol/g) were used for the coupling cycles, using commercial 3'-*O*-(2-cyanoethyl)-*N*,*N*-diisopropylphosphoramidite nucleosides and **5** as building blocks in concentration of 40 mg/mL. Coupling efficiences, checked by spectroscopic DMT test, were always superior to 98 %. For the synthesis and purification of the natural DNA and RNA oligomers standard procedures[20,21] were followed.

Deprotection, Purification and Characterization of Natural and Modified Oligomers a-d.

Once DNA synthesis was completed CPG resin was dried and transferred into a screw-cap vial and suspended in 1.5 mL of concentrated NH_4OH for 6 h at 55 °C. The supernatant was filtered and the support was washed with water. The combined filtrate and washings were concentrated under reduced pressure, redissolved in water and analyzed by HPLC. Ferrocenyl-ODNs **a-d** were purified on a Partisil 10 SAX column (Whatman, 4.6 × 250 mm, 7 μm) eluted with linear gradients of aq. solution of KH_2PO_4 (20% CH_3CN, v/v, pH = 7.0) from 1.0 to 350 mM in 30 min, flow 0.7 mL/min showing the following retention times: **a** = 25.7 min, **b** = 26.5 min, **c** = 24.6 min, **d** = 24.7 min. Ferrocene free-oligos 17-mers and 16-mers were purified on a Nucleogen DEAE 60-7 Macherey-Nagel column (4.0 × 125 mm, 7 μm); buffer A: 20 mM K_2HPO_4 aq. solution, pH 7.0, containing 20 % (v/v) CH_3CN; buffer B: 1 M KCl, 20 mM K_2HPO_4 aq. solution, pH = 7.0, containing 20% (v/v) CH_3CN, using a linear gradient from 10 to 100 % B in 30 min, flow 0.8 mL/min. The isolated oligomers were successively desalted by gel filtration on a Sephadex G25 column eluted with H_2O. By HPLC analysis on a Waters μBondapak™ RP18 analytical column (Millipore, 300 × 3.9 mm, 5 μm), they resulted to be more than 98 % pure. Using a linear gradient (from 0 to 50 % in 30 min) of CH_3CN in 0.1 N aq. triethylammonium bicarbonate buffer pH = 7.0 (flow 0.8 mL/min, detection at λ = 260 nm), ferrocenyl-ODNs **a-d** showed the following retention times: **a**: 18.6 min, **b**: 17.9 min (ferrocene-free 17-mer retention time: 15.7 min), **c**: 18.5 min, **d**: 17.9 min (ferrocene-free 16-mer retention time 15.1 min). The synthesized oligomers **a-d** were characterized by MALDI TOF MS: oligonucleotides **a** and **b**, mass calculated $[M-H]^-$ = 5443, mass observed = 5444; oligonucleotides **c** and **d**, mass calculated $[M-H]^-$ = 4960, mass observed 4962.

Thermal denaturation experiments.

The concentration of the synthesized ODNs was determined spectrophotometrically at λ = 260 nm and at 85 °C, using the following molar extinction coefficients for each base:[38] 15400, 11700, 8800, 7300 $cm^{-1} M^{-1}$ for A, G, T, C respectively in the denaturated state. A 100 mM NaCl, 10 mM NaH_2PO_4 aq. solution at pH = 7.0 was used for duplexes melting experiments; for triplexes a 140 mM KCl, 5 mM $MgCl_2$, 5 mM NaH_2PO_4 aq. solution at 5.5 and 6.0 pH values was used. Melting curves were recorded using a concentration of 2 μM and 1.21 μM (respectively for duplex and triplex experiments) for each strand in 1 mL of the tested solution in Teflon stoppered quartz cuvettes of 1 cm optical path length. The resulting solutions were then allowed to heat at 80 °C for 15 min, then slowly cooled and kept at 5 °C for 20 min. After thermal equilibration at 20 °C, UV absorption at λ = 260 nm was monitored as a function of the temperature, increased at a rate of 0.5 °C/min, typically in the range 20-80 °C. The temperatures relative to the duplex melting, reported in Table 1, were determined as the maxima of the first derivative of absorbance *vs.* temperature plots.

Circular Dichroism Spectroscopy

Buffer and sample conditions were the same as those used for UV thermal analysis studies. Quartz cells with path length of 1 cm were used. CD spectra were run at 20 °C, adjusted with a circulating water bath, in the

spectral window from 205 to 350 nm (single strands and duplex measurements) or from 205 to 330 nm (triplex measurements). CD melting experiments were carried out at λ = 220 nm. CD was monitored as a function of the temperature, increased at a rate of 1 °C/min, in the range 20-80 °C. The temperatures relative to triplex melting, reported in Table 1, were determined as the maxima of the first derivative of CD *vs.* temperature plots.

Acknowledgements

The authors are grateful to MURST and CNR for grants in support of this investigation, to C.I.M.C.F., Università di Napoli "Federico II" for NMR facilities. They also thank Prof. Carlo Pedone for a critical reading of the manuscript and Rita Carolla and Leopoldo Zona for competent technical assistance.

References

1. Köpf-Maier, P.; Köpf, H.; Neuse, E.W. *Angew. Chem. Int. Ed. Engl.*, **1984**, *23*, 456-457.
2. Farrel, N. *Transition Metal Complexes as Drugs and Chemotherapeutic Agents*, Kluwert Academic Publishers, Dordrecht, 1989.
3. Köpf-Maier; P., Köpf, H. *Chem. Rev.*, **1987**, *87*, 1137-1152.
4. Scaria, V.; Furlani, A.; Longato, B.; Corain, B.; Pilloni, G. *Inorg. Chim. Acta*, **1988**, *153*, 67-70.
5. Hill, D.T.; Girard, G.R.; McCabe, F.L.; Johnson, R.K.; Stupik, P.D.; Zhang, J.K.; Reiff, W.M.; Eggleston, D.S. *Inorg.Chem.*, **1989**, *28*, 3529-3533.
6. Neuse, E.W.; Meirim, M.G.; Blom, M.F. *Organometallics*, **1988**, *7*, 2562-2565.
7. Houlton, A.; Roberts, M.G.; Silver, J. *J. Organomet. Chem.*, **1991**, *418*, 107-112.
8. Murray, J.H., Harding, M.M. *J. Med. Chem.*, **1984**, *37*, 1936-1941.
9. Köpf-Maier, P., Preiss, F.; Marx, T.; Klapötke, T.; Köpf, H. *Anticancer Res.*, **1986**, *6*, 33-37.
10. Köpf-Maier, P.; Moormann, A.; Köpf, H. *Eur. J. Cancer Clin. Oncol.*, **1985**, *21*, 853-858.
11. Köpf-Maier, P.; Köpf, H., Neuse, E.W. *J. Cancer Res. Clin. Oncol.*, **1984**, *108*, 336-340.
12. Price, C.; Aslanoglu, M.; Isaac, C.J.; Elsegood, M.R.J.; Clegg, W.; Horrocks, B.R.; Houlton, A. *J. Chem. Soc., Dalton Trans.*, **1996**, 4115-4120.
13. Meunier, P.; Quattara, I., Gautheron, B., Tirouflet, J., Camboli, D., Besançon, J. *Eur. J. Med. Chem.*, **1991**, *26*, 351-362.
14. Takenaka, S.; Uto, Y., Kondo, H., Ihara, T., Takagi, M. *Anal. Biochem.*, **1994**, *218*, 436-443.
15. Jacobson, K.B.; Arlinghaus, H.F.; Schmitt, H.W.; Sachleben, R.A.; Brown, G.M.; Thonnard, N.; Sloop, F.V.; Foote, R.S.; Larimer, F.W.; Woychik, R.P. *Genomics*, **1991**, *9*, 51-59.
16. Ihara, T.; Nakayama, M.; Murata, M.; Nakano, K.; Maeda, M. *Chem. Commun.*, **1997**, 1609-1610.
17. Keller, G.H.; Manak, M.M. *DNA Probe*, Stockton Press, London, 1990.
18. Ihara, T.; Maruo, Y.; Takenaka, S.; Takagi, M. *Nucleic Acids Res.*, **1996**, *24*, 4273-4280.
19. Mucic, R.C.; Herrlein, M.K.; Mirkin, C.A.; Letsinger, R.L. *Chem. Commun.*, **1996**, 555-557.

20. Gait, M.J. Ed., *Oligonucleotide Synthesis: A Practical Approach*, IRL Press, Washington, DC, pp 35-81, 1990.
21. Eckstein, F. Ed., *Oligonucleotides and Analogues: a Practical Approach*, IRL Press, Oxford, U.K., pp 1-23, 1991.
22. Uhlmann, E.; Peyman, A. *Chem. Rev.*, **1990**, *90*, 543-583.
23. De Napoli, L.; Messere, A.; Montesarchio, D.; Piccialli, G.; Benedetti, E.; Bucci, E.; Rossi, F. *Bio. Med. Chem.*, **1999**, *7*, 395-400.
24. Lin, S.B.; Kao, C.F.; Lee, S.C.; Kan, L.S. *Anticancer Drug. Des.*, **1994**, *9*, 1-8.
25. Thuong, N.T.; Hélène, C. *Angew. Chem. Int. Ed. Engl.* **1993**, *32*, 666-690.
26. Walker, T.; De Clercq, E.; Eckstein, F. Eds. *Nucleoside Analogues, Chemistry, Biology and Medical Applications*, Plenum Press; New York and London, p 169, 1979, and references therein.
27. For a review see: Mitsunobu, O. *Synthesis*, **1981**, 1-28.
28. Tsunoda, T.; Yamamiya, Y.; Itô, S. *Tetrahedron Lett.*, **1993**, *34*, 1639-1642.
29. De Napoli, L.; Mayol, L.; Piccialli, G.; Rossi, M.; Santacroce, C. *J. Heterocyclic Chem.*, **1986**, *23*, 1401-1403.
30. Bischofberger, N. *Tetrahedron Lett.*, **1987**, *28*, 2821-2824.
31. De Napoli, L.; Messere, A.; Montesarchio, D.; Piccialli, G.; Santacroce, C. *Bio. Med. Chem. Lett.*, **1992**, *2*, 315-318.
32. Greeve, J.; Maestre, M.F.; Levin, A. *Biopolymers*, **1977**, *16*, 1489-1504.
33. Saenger, W. *Principles of Nucleic Acid Structure*, Springer-Verlag, p 258, 1983.
34. Kan, L.S.; Callahan, D.E.; Trapane, T.L.; Miller, P.S.; Ts'o, P.O.; Huang, D.H. *J. Biomol. Struct. Dyn.*, **1991**, *8*, 911-933.
35. Lee, J.S.; Johnson, D.A.; Morgan, A.R. *Nucl. Acids Res.*, **1979**, *6*, 3073-3091.
36. Gray, D.M.; Ratliff, R.L.; Antao, V.P.; Gray, C.W. in Sarma, R.H. and Sarma, M.H. (Eds.), *Structure and Expression, Vol. 2: DNA and Its Drug Complexes*, Adenine Press, pp.147-165, 1987.
37. Antao, V.P.; Gray, D.M.; Ratliff, R.L. *Nucl. Acids Res.*, **1987**, *16*, 719-738.
38. Beal, P.A.; Dervan, P.B. *J. Am. Chem. Soc.*, **1992**, *114*, 4976-4982.